Understanding fractional-order surface plasmons

Yuping Yang[1,2] and Daniel Grischkowsky[1,*]

[1]*School of Electrical and Computer Engineering, Oklahoma State University, Stillwater, Oklahoma 74078, USA*

[2]*School of Science, Minzu University of China, Beijing 100081, China*

**Corresponding author: daniel.grischkowsky@okstate.edu*

Received August 17, 2011; revised September 19, 2011; accepted September 21, 2011;
posted September 21, 2011 (Doc. ID 153016); published October 26, 2011

We show experimentally that diffraction-induced surface plasmon excitation can mimic enhanced transmission and cause a highly sensitive modulation by the coherent interference between zero-order and reflected first-order diffraction in select regions of the terahertz spectrum. Based on the study of a one-dimensional metallic grating, we obtain the physical mechanisms of the fractional-order surface plasmon resonances observed with the two-dimensional grating of the metallic hole array. © 2011 Optical Society of America

OCIS codes: 240.6680, 300.6495, 050.6624.

Recently, a new type of extremely sharp resonant lines between the fundamental surface plasmon modes of a hole array fabricated on high-resistivity silicon wafers in "optical contact" with thick silicon plates has been reported [1]. Therein, these "sharp lines" were called "fractional-order surface plasmons (FSP)" and were simply explained in terms of coupling between the standing surface waves and the terahertz (THz) waves transmitted through the hole pattern. Here, we report new experimental observations showing that the FSP resonances disappear with complete optical contact.

Supported by the observations in Fig. 1, we will show that the FSP resonances are caused by the surprisingly large reflections from gaps as thin as 1 μm between the backside of the hole array wafer and the thick backing plate. However, as shown in Fig. 2, this is not just the small reflection from the zero-order transmission pulse from the two-dimensional (2D) diffraction grating of the hole array. The total reflection in the zero-order forward direction also includes strong first-order reflected beams. When incident on the backside of the hole array, these reflected first-order beams are mainly transmitted through the hole array, counterpropagating with respect to the incident beam. Most importantly, due to the dielectric interface on the holes of the 2D hole-array grating, a strong coherent reflection occurs in the zero-order forward direction. This first-order reflection interferes with the zero-order reflection and with the long duration THz zero-order, ring-down radiation of the hole-array resonances. The interference between these three THz beams leads to the sharp FSP features in the transmitted spectrum.

The measurements presented in Fig. 1 used the THz time domain spectroscopy technique to measure the THz electric field pulse with subpicosecond time resolution [2]. For this characterization a subpicosecond THz pulse was incident on the hole array. The measured transmitted THz pulse consists of the attenuated subpicosecond pulse due to the classical transmission of the array, followed by the dramatic ringing structure, which can extend as long as 250 ps due to the FSP resonances excited by the incident pulse. Here, the metal film hole array is a lithographically fabricated 280 nm thick Al layer deposited on the front side of a double-sided polished 0.45 mm thick, 400 $\Omega \cdot$ cm resistivity Si wafer. The 60 μm period of the hole array has the rectangular hole dimensions of 15 μm (x axis) $\times$30 μm (y axis). A 10 mm thick, high-resistivity Si plate was placed in contact with the backside of the wafer to eliminate the backside reflection, thereby enabling observations to 250 ps. The amplitude transmission of the sample wafer with the backing plate was obtained by dividing the amplitude spectrum of the transmitted (sample) pulse by the amplitude spectrum of the reference pulse transmitted through only the Si backing plate.

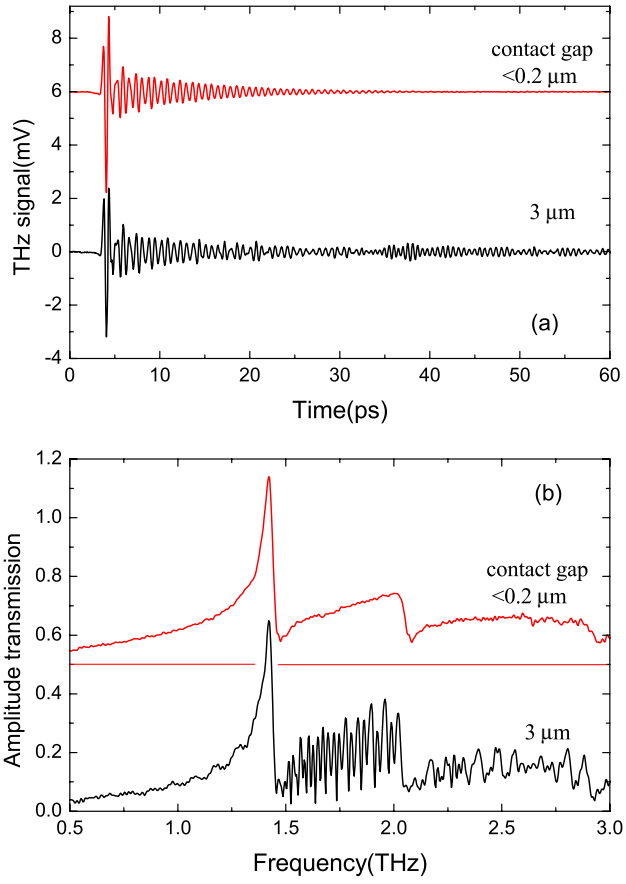

Fig. 1. (Color online) Measured transmitted THz pulses through the hole array in contact with a 10 mm Si backing plate. (a) Upper trace, optical contact (gap < 0.2 μm) to Si plate. Lower trace, incomplete (3 μm gap) contact to a 3 mm Si plate. (b) Amplitude transmission spectra of upper and lower THz pulses.

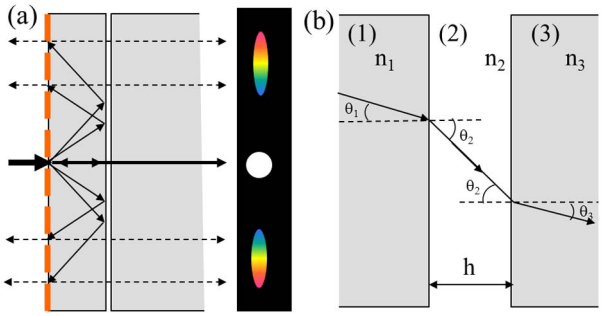

Fig. 2. (Color online) (a) Cross-section diagram showing the zero-order direct transmission through the (1D) grating (red) and the first-order diffraction beams reflecting from the gap and back to the grating, where they are diffracted in the backward direction; the dielectric interface causes a partial reflection in the zero-order forward direction. (b) Diagram showing path and angles used in the calculated reflections from the gap.

For the complete contact case, the clean ringdown signal corresponds to the three fundamental SP resonances shown in Fig. 1(b). However, with an incomplete 3 μm gap contact to a 3 mm thick Si plate, a much more complicated and longer-lasting signal is obtained with the narrow line structure of the FSP resonances. The effective gap thickness is determined from the amplitude of the reflected gap signal that occurs before the first zero-order-reflected THz pulse from the backside of the Si plate. This gap-measuring (GM) reflection for both the 2D and 1D transmission gratings is observed by a long duration time scan of the THz output pulse, which includes the first reflection. The ratio of the GM reflection to the first zero-order reflection provides the best measure of the gap.

An analysis of the original FSP data files [1] showed a GM reflection with an amplitude indicating a 3 μm gap. In contrast, for the complete contact signal in Fig. 1(a), the amplitude of the GM reflection was too small to measure, indicating a less than 0.2 μm gap. An additional indicator of complete optical contact is the lack of oscillatory structure in the amplitude spectrum below the first SP resonance. The original FSP observation [1] showed oscillatory structure similar to that shown in Fig. 1(b) for the 3 μm gap; here, complete contact shows no structure.

We will now show that the effect of THz gap reflection is much enhanced for a 1D metallic transmission grating on Si. Furthermore, the first-order reflection is as strong as that for the zero order. Here, the 1D grating with a period of 100 μm, consisted of 75 μm Al lines separated by 25 μm. The 280 nm thick Al film grating was fabricated by photolithography on a double-sided polished 0.36 mm thick high-resistivity Si wafer. A 3 mm thick, high-resistivity Si plate was placed in contact with the backside of the grating wafer. The THz input pulses were linearly polarized (horizontal) and at normal incidence to the vertical lines of the grating.

Figure 3(a) shows the THz pulses transmitted in the zero-order direction of the grating, with different gaps. There is an extremely sensitive dependence to the gap, indicated by the small gap reflection (R0) occurring in the transmitted pulse at the position of the dashed line. Again, the main effect of the gap is not the small reflection R0 of the zero-order transmitted pulse, but the initiation of the much stronger reflection of the first-order diffracted THz beams (labeled R1) from the gap. It is important to note that R1 describes a frequency swept (chirped) pulse with the highest frequency right after the R0 reflection, followed by a long duration oscillation with a monotonically increasing period. This result is consistent with the first-order path increasing with wavelength.

The first-order round trip paths from the transmission grating to the gap and reflecting back to the 1D grating are longer than 14 wavelengths (in silicon) for frequencies above the SP mode at 0.88 THz. Although this is relatively short for Fraunhofer ray analysis, the requirement (with only one possible optical path) of diffraction and then partial reflection into the zero-order forward direction is considered to justify our analysis.

The first-order reflection occurs at angles beyond the critical angle $\theta_c = \arcsin(1/n) = 17.0°$, for silicon with the high THz index of refraction $n = 3.42$. In our collinear mounting ($\theta_i = 0$), the first-order diffraction angle is $\theta_1 = \arcsin(\lambda_0/nP)$, with λ_0 the free-space wavelength, P the grating periodicity (100 μm), and $n = 3.42$. The angle of diffraction θ_1 tracks wavelength; shorter wavelengths appear nearest to the zero-order direction and the longer wavelengths appear at larger angles, as in Fig. 2(a). The fundamental [0,1] SP mode has the free-space wavelength $\lambda_{sp} = nP$ (0.88 THz) [3,4].

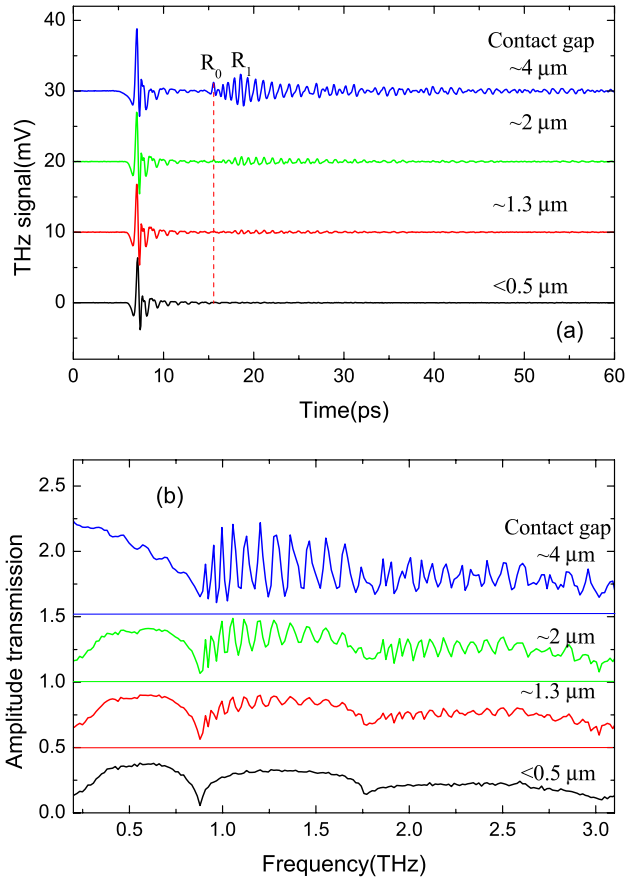

Fig. 3. (Color online) (a) Measured THz pulses transmitted through the (1D) diffraction grating with different gaps between the grating wafer and the 3 mm Si backing plate. (b) Amplitude transmission spectra of the transmitted pulses.

A simplified understanding of the FSP resonances above the SP mode at 0.88 THz is based on the interference between the first-order reflection into the zero-order direction, the zero-order reflection and the zero-order direct transmission. With respect to the zero-order direct transmission, the round trip path difference in Si wavelengths for the first order is $N_\lambda^{1R} = 2L\,n/(\lambda_o \cos\theta_1)$, and for the zero-order reflection is $N_\lambda^{0R} = 2L\,n/\lambda_o$. For an integral number of wavelengths, these reflected waves are in phase with the zero-order transmission and out of phase for an integer plus 0.5. Similarly, for $(N_\lambda^{1R} - N_\lambda^{0R})$ equal to an integer the two reflected waves are in phase with each other and out of phase for an integer +0.5. In agreement with Fig. 3, this qualitative model has eight in-phase resonances between 1.0 and 1.5 THz, which become closer together at lower frequencies.

We will now compare the zero-order and the first-order (beyond the critical angle) gap reflections. The reflection from the gap as shown in Fig. 2(b), is given by [5,6]

$$r = \frac{r_{12} + r_{23}e^{2i\beta}}{1 + r_{12}r_{23}e^{2i\beta}}, \beta = \frac{2\pi}{\lambda_0} n_2 h \cos\theta_2,$$

with

$$r_{12} = \frac{n_1\cos\theta_1 - n_2\cos\theta_2}{n_1\cos\theta_1 + n_2\cos\theta_2}, r_{23} = \frac{n_2\cos\theta_2 - n_3\cos\theta_3}{n_2\cos\theta_2 + n_3\cos\theta_3}.$$

For our case, $n_3 = n_1$, $r_{12} = -r_{21}$, and r becomes

$$r = \frac{r_{12}(1 - e^{2i\beta})}{1 - r_{12}^2 e^{2i\beta}}. \quad (1)$$

For normal incidence with $\theta_1 = \theta_2 = \theta_3 = 0$ and $2\beta \ll 1$, r is given to first order in 2β as $r = -i2\beta r_{12}/[1 - (r_{12})^2]$, which becomes $r = -i9.56\,\mathrm{h}/\lambda_o$.

When θ_1 is larger than the critical angle, the reflection can be written in a similar form as

$$r = \frac{r_{12} + r_{23}e^{-2b}}{1 + r_{12}r_{23}e^{-2b}}, \quad \text{with } ib = k_0 h n_2 \cos\theta_2 \quad (2)$$

and $n_2\cos\theta_2 = -i(n_1^2\sin^2\theta_1 - 1)^{0.5}$. The exponential falloff of the evanescent field from the Si surface is described by b and is important in understanding the recent THz optical tunneling experiments [6]. r_{12} and r_{23} have their previous above form, but with the above complex expression for $n_2\cos\theta_2$. For our case with $n_3 = n_1$ and $r_{12} = -r_{23}$, r becomes

$$r = \frac{r_{12}(1 - e^{-2b})}{1 - r_{12}^2 e^{-2b}}. \quad (3)$$

It is easily shown that r_{12} can be written as $r_{12} = e^{-i2\varphi}$, where φ is given by

$$\varphi = \arctan\left[\left(\sqrt{n_1^2\sin^2\theta_1 - 1}\right)/n_1\cos\theta_1\right]. \quad (4)$$

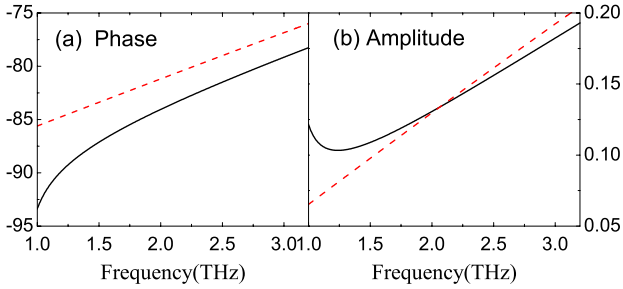

Fig. 4. (Color online) Calculated phase angle in (a) degrees and amplitude (b) for the complex reflections r of a 2 μm gap for the zero-order (dashed line) and first-order (solid line) transmitted beams from the grating.

We then obtain

$$r = \frac{e^{-i2\varphi}(1 - e^{-2b})}{1 - e^{-i4\varphi}e^{-2b}} = \frac{(1 - e^{-2b})}{e^{i2\varphi} - e^{-i2\varphi}e^{-2b}}. \quad (5)$$

Using the above results, we compare in Fig. 4 the calculated complex reflections from a 2 μm gap for the zero-order and first-order THz beams from the 100 μm grating at normal incidence. The first-order reflection is significantly larger than the zero order for frequencies below 1.5 THz, after which they are comparable up to 3 THz.

In summary, the FSPs have been shown to occur only with the reflection from a small gap between the backside of a 2D hole-array transmission grating or a 1D grating wafer and the attached backing plate. The FSP resonances are much stronger for a 1D grating compared to the 2D hole array. The FSP resonances are caused by the gap reflection of the zero-order and the first-order diffracted beams back to the 1D or 2D grating, where there is a partial reflection into the forward zero-order direction, thereby causing the sharp interference peaks identified as the FSP resonances. This effect shows the importance of considering the 1D or 2D diffracted beams together with the zero-order transmission, when interpreting transmission measurements.

We acknowledge experimental support from S. Sree Harsha and Alisha J. Shutler, and a careful reading of this manuscript by John O'Hara. This work was supported by the U.S. National Science Foundation (NSF), the National Natural Science Foundation of China (NSFC) (grant 11104360), and the "985 Project" (grants 98503-008006, 98503-008017) of Ministry of Education of China.

References

1. D. Qu and D. Grischkowsky, Phys. Rev. Lett. **93**, 196804 (2004).
2. D. Grischkowsky, S. Keiding, M. van Exter, and C. Fattinger, J. Opt. Soc. Am. B **7**, 2006 (1990).
3. T. W. Ebbesen, H. J. Lezec, H. F. Ghaemi, T. Thio, and P. A. Wolff, Nature **391**, 667 (1998).
4. D. Qu, D. Grischkowsky, and W. Zhang, Opt. Lett. **29**, 896 (2004).
5. M. Born and E. Wolf, *Principles of Optics*, 7th ed. (Cambridge University, 1999), pp. 49–51 and 64–70.
6. M. T. Reiten, D. Grischkowsky, and R. A. Cheville, Phys. Rev. E **64**, 036604-1 (2001).